◆ Human Brain Mapping 33:1700–1716 (2012) ◆

Brain Systems for Baroreflex Suppression During Stress in Humans

Peter J. Gianaros,[1]* Ikechukwu C. Onyewuenyi,[2] Lei K. Sheu,[1] Israel C. Christie,[1] and Hugo D. Critchley[3,4,5]

[1]*Department of Psychiatry, University of Pittsburgh, Pittsburgh, Pennsylvania*
[2]*Department of Psychology, University of Pittsburgh, Pittsburgh, Pennsylvania*
[3]*Department of Psychiatry, Brighton and Sussex Medical School, University of Sussex, Brighton, United Kingdom*
[4]*Sackler Centre for Consciousness Science, University of Sussex*
[5]*Sussex Partnership NHS Foundation Trust*

Abstract: The arterial baroreflex is a key mechanism for the homeostatic control of blood pressure (BP). In animals and humans, psychological stressors suppress the capacity of the arterial baroreflex to control short-term fluctuations in BP, reflected by reduced baroreflex sensitivity (BRS). While animal studies have characterized the brain systems that link stressor processing to BRS suppression, comparable human studies are lacking. Here, we measured beat-to-beat BP and heart rate (HR) in 97 adults who performed a multisource interference task that evoked changes in spontaneous BRS, which were quantified by a validated sequence method. The same 97 participants also performed the task during functional magnetic resonance imaging (fMRI) of brain activity. Across participants, task performance (i) increased BP and HR and (ii) reduced BRS. Analyses of fMRI data further demonstrated that a greater task-evoked reduction in BRS covaried with greater activity in brain systems important for central autonomic and cardiovascular control, particularly the cingulate cortex, insula, amygdala, and midbrain periaqueductal gray (PAG). Moreover, task performance increased the functional connectivity of a discrete area of the anterior insula with both the cingulate cortex and amygdala. In parallel, this same insula area showed increased task-evoked functional connectivity with midbrain PAG and pons. These novel findings provide human evidence for the brain systems presumptively involved in suppressing baroreflex functionality, with relevance for understanding the neurobiological mechanisms of stressor-related cardiovascular reactivity and associated risk for essential hypertension and atherosclerotic heart disease. *Hum Brain Mapp 33:1700–1716, 2012.*

Key words: amygdala; baroreflex; cingulate cortex; insula; stress

Additional Supporting Information may be found in the online version of this article.

Contract grant sponsor: National Institutes of Health; Contract grant number: R01-HL089850; Contract grant sponsor: Pennsylvania Department of Health.

*Correspondence to: Peter J. Gianaros, Department of Psychiatry, University of Pittsburgh, 3811 O'Hara Street, Pittsburgh, PA 15213. E-mail: gianarospj@upmc.edu

Received for publication 18 November 2010; Revised 6 March 2011; Accepted 7 March 2011

DOI: 10.1002/hbm.21315

Published online 12 May 2011 in Wiley Online Library (wileyonlinelibrary.com).

INTRODUCTION

Acute psychological stressors evoke cardiovascular reactions that provide hemodynamic and metabolic support for contextually adaptive behavior [Obrist, 1981]. Core components of such cardiovascular reactions include simultaneous increases in blood pressure (BP) and heart rate (HR) [Kamarck and Lovallo, 2003]. However, while stressor-evoked cardiovascular reactions can be adaptive in the short-term, the recurrent expression of large-magnitude or metabolically "exaggerated" stressor-evoked cardiovascular reactions by some individuals can be maladaptive in the long-term. Hence, individuals who exhibit large-magnitude stressor-evoked cardiovascular reactions are at risk for hypertension, premature atherosclerosis, ventricular enlargement, stroke, and myocardial infarction [Chida and Steptoe, 2010].

Cardiovascular reactions to psychological stressors are orchestrated by a network of cortical and subcortical brain regions, particularly regions of the cingulate cortex, insula, amygdala, and midbrain periaqueductal gray (PAG) [Allen et al., 1991; Cechetto, 1994; Dampney, 1994; Gianaros and Sheu, 2009; Heimer and van Hoesen, 2006; Neafsey, 1990; Resstel and Correa, 2006; Saha, 2005; Ulrich-Lai and Herman, 2009; Verberne and Owens, 1998; Wager et al., 2009b; Wang et al., 2005; Yasui et al., 1991]. Together, these brain regions support the processing of salient environmental stimuli that are unpredictable, uncontrollable, conflictual, aversive, and thus labeled as psychologically stressful [McEwen and Gianaros, 2011]. Moreover, convergent animal and human evidence links these brain regions to the generation of acute cardiovascular reactions to stressful stimuli, ultimately reflecting their influence on brainstem nuclei that control autonomic nerve traffic to the myocardium and vasculature [Dampney, 1994; Verberne and Owens, 1998]. Critically, a key mechanism by which the processing of psychological stressors evokes acute cardiovascular reactions (e.g., simultaneous BP and HR rises) involves the central nervous system suppression of the arterial baroreflex [Berntson et al., 1998; Dampney, 1994; Gianaros and Sheu, 2009; Neafsey, 1990; Saha, 2005; Verberne and Owens, 1998].

The arterial baroreflex is a homeostatic mechanism that constrains oscillations in beat-to-beat BP around a regulatory set-point by rapidly adjusting HR, cardiac contractility, and vascular resistance through coordinated and negative-feedback changes in autonomic nervous system activity [Eckberg and Sleight, 1992]. The homeostatic control of BP by the baroreflex depends on afferent signaling from stretch-sensitive mechanoreceptors (baroreceptors) that are densely concentrated in the vessel walls of the carotid arteries and aortic arch [Dampney, 1994; Dampney et al., 2002]. In response to rises in BP that expand vessel walls, baroreceptors increase their firing frequency. This firing is relayed centrally along vagal and glossopharyngeal nerve bundles to the nucleus tractus solitarius (NTS), where baroafferent signals are then relayed to parasympathetic (e.g., nucleus ambiguus, dorsal motor nucleus) and sympathetic (e.g., caudal and rostral ventrolateral medulla) source nuclei. Engagement of these autonomic source nuclei in turn decreases HR, cardiac contractility, and vascular resistance, which serve to return arterial BP toward a regulated set-point in a homeostatic, control-loop fashion [Dampney, 1994].

During the processing of psychological stressors by cortical and subcortical brain systems, however, there is a suppression of the capacity of the baroreflex to regulate BP through homeostatic (negative-feedback) processes. This stressor-evoked suppression of baroreflex sensitivity (BRS) is apparent in the relationship between heart beat interval and BP adjustments following successive (beat-to-beat) changes in BP [Berntson et al., 1998; Dampney, 1994; Neafsey, 1990]. In animals, it is well established that the stressor-evoked engagement of cortical and subcortical brain regions can suppress the baroreflex via their influences brainstem nuclei directly involved in autonomic cardiovascular control [Berntson et al., 1998; Cechetto, 1994; Dampney, 1994; Neafsey, 1990; Verberne and Owens, 1998]. In humans, the processing of psychological stressors by putatively homologous brain regions is also suggested to act upon autonomic source nuclei to reduce parasympathetic cardiac control and redirect sympathetic vascular outflow, allowing (i) BP to exceed a regulated set-point and (ii) HR and BP to rise simultaneously, with such cardiovascular reactions being exaggerated and possibly pathogenic in some individuals [Gianaros and Sheu, 2009; Obrist, 1981]. Hence, it is has been hypothesized that through their influence on baroreflex functionality, particular cortical and subcortical brain regions may directly contribute to emergent individual differences in stressor-evoked cardiovascular reactivity and associated cardiovascular disease risk [Berntson et al., 1998]. At present, however, there are no published human studies that address whether activation in cortical or subcortical regions (directly coupled to brainstem nuclei involved in autonomic cardiovascular control) predicts individual differences in the magnitude of BRS changes during psychological stress. This knowledge gap contrasts with a corpus of animal evidence demonstrating that cortical and subcortical regions, particularly within the cingulate cortex, insula, amygdala, and midbrain PAG, affect baroreflex functionality during behavioral states of stress [Berntson et al., 1998; Cechetto, 1994; Dampney, 1994; Neafsey et al., 1993; Resstel and Correa, 2006; Saha, 2005; Schlor et al., 1984].

Accordingly, we used functional magnetic resonance imaging (fMRI) to test the first hypothesis that individual differences in the stressor-evoked suppression of BRS covary with regional brain activity within the cingulate, insula, amygdala, and midbrain PAG. To this end, otherwise healthy midlife adults ($n = 97$) performed a modified version of a multisource interference task (MSIT) [Bush and Shin, 2006], which involves processing conflictual information, receiving negative feedback, and making time-pressured responses to unpredictable stimuli that evoke psychological distress and cardiovascular reactivity [Gianaros et al., 2009]. We next tested the second hypothesis that during task performance, the perigenual region of the anterior cingulate cortex (pACC) and amygdala would

exhibit increased functional connectivity (taken to reflect the quantitative strength of time-dependent and contextually modulated covariation in neural activity across brain areas) [Friston, 1994; Friston et al., 1997] with the insula. As described below, this hypothesis was based on our present understanding of the anatomical connections and functional interactions between these particular regions in the context of autonomic cardiovascular control [Cechetto, 1994; Cechetto and Shoemaker, 2009; Dampney, 1994; Verberne et al., 1987; Verberne and Owens, 1998; Vogt, 2005]. Finally, we tested the third hypothesis that task performance would increase the functional connectivity of the insula with midbrain (PAG) and brainstem (pons) regions (i) known to be involved in baroreflex regulation and (ii) amenable to assessment using conventional fMRI methods [Gray et al., 2009a]. The latter two hypotheses are further supported by recent evidence indicating that the pACC and amygdala in particular play key functional roles in mediating individual differences in stressor-evoked BP reactivity, consistent with their direct and indirect projections to insular and preautonomic cell groups [Cechetto and Shoemaker, 2009; Dampney, 1994; Vogt, 2005] that regulate baroreflex functionality [Gianaros and Sheu, 2009; Gianaros et al., 2008]. Further, the insula is widely regarded as "limbic integration cortex" [Augustine, 1996], because of its dense connections with rostral portions of the anterior cingulate abutting the genu of the corpus callosum, amygdalar subdivisions, and other networked paralimbic brain areas important for evaluative processing and for adaptively responding to behaviorally salient or otherwise stressful environmental stimuli [Barbas et al., 2003; Berntson et al., 2011; Cauda et al., 2011; Öngür and Price, 2000; Seeley et al., 2007]. Finally, the insula issues and receives dense projections to and from midbrain and brainstem regions that regulate autonomic source nuclei that influence peripheral target organs (e.g., the heart and vasculature) [Augustine, 1996; Cechetto, 1994; Öngür and Price, 2000; Verberne and Owens, 1998]. Importantly, such insular projections are understood to integrate interoceptive (e.g., baroafferent) information with the processing of environmental and stressful stimuli in the service of coordinating cardiovascular function with contextually adaptive behavior [Allen et al., 1991; Cechetto, 1994; Nagai et al., 2010]. Moreover, lesion, stimulation, neuroanatomical tracing, and in vivo neuroimaging evidence strongly implicates the insula in the integrative and homeostatic control over cardiovascular physiology [Allen et al., 1991; Cechetto, 1994; Cechetto and Chen, 1990; Cechetto and Shoemaker, 2009; Oppenheimer, 1993; Ruggiero et al., 1987; Verberne and Owens, 1998; Yasui et al., 1991].

METHODS

Participants

Participants were 47 men (mean age = 39.9 ± 6.2 SD) and 50 women (mean age = 40.2 ± 6.1 SD) recruited by mass mailings to residents of Allegheny County, Pennsylvania, USA. Those responding to mailings were screened to exclude those with (i) a history of cardiovascular disease (including treatment for or diagnoses of hypertension, stroke, myocardial infarction, congestive heart failure, and atrial or ventricular arrhythmias); (ii) prior cardiovascular surgery (including coronary bypass, carotid artery, or peripheral vascular surgery); (iii) chronic kidney or liver conditions, Type I or II diabetes, or any pulmonary or respiratory diseases; (iv) current psychiatric diagnoses of a substance abuse or mood disorder (including alcohol dependence, a somatization disorder, major depression or a subclinical depressive syndrome, and panic or other anxiety disorders), as confirmed on interview using the Patient Health Questionnaire [Spitzer et al., 1999], an inventory validated in outpatient [Kroenke et al., 2001; Lowe et al., 2004a; Spitzer et al., 1999] and community samples [Martin et al., 2006] for sensitivity and specificity against the Diagnostic and Statistical Manual of Mental Disorders IV [Lowe et al., 2004b]; (v) prior cerebrovascular trauma involving loss of consciousness; (vi) prior neurosurgery or any neurological condition; (vii) being pregnant (verified by urine test in females); (viii) having claustrophobia or metallic implants; or (ix) taking psychotropic, lipid lowering, or cardiovascular medications.

Of those meeting the above criteria, 66 participants reported being of Caucasian descent. Remaining participants reporting being of African–American descent (n = 20), Asian descent (n = 4), Eastern Mediterranean decent (n = 1), Indian decent (n = 1), and multiracial descent (n = 2) (three individuals did not endorse any category of ethnicity). Prior to testing, participants also completed inventories to characterize depressive symptoms, dispositional anxiety and hostility, as well as recent levels of life stress experienced in the past month. These inventories included the Beck Depression Inventory (BDI-II) [Beck et al., 1996], and the trait versions of the Spielberger State-Trait Anxiety Inventory (STAI-T) [Spielberger et al., 1970], the Cook–Medley Hostility Scale (CMHS) [Barefoot et al., 1989; Cook and Medley, 1954], and the Perceived Stress Scale (PSS, 10-item version) [Cohen et al., 1983]. Scores on these inventories did not correlate significantly with resting BRS or with stressor-evoked changes in BRS (r's ranged from −0.103 to −0.002, all $Ps \geq 0.32$). Finally, participants reported consuming a median of one alcoholic beverage per week (range = 0–14 beverages/week). In this sample, alcohol consumption was not significantly correlated with resting BRS or with stressor-evoked changes in BRS (Spearman rho's range: −0.03 to −0.05, all $Ps \geq 0.63$). Given the above null findings, negative emotionality, life stress, and alcohol consumption variables are unlikely to have explained or confounded study findings and were thus not considered further. Participants' average, seated resting systolic BP (SBP)/diastolic BP (DBP) was 120.3/72.6 mm Hg (±9.4/9.2 SD), as determined by the mean of the last two of three BPs obtained

TABLE I. Summary of participant characteristics

Characteristic	Mean or (%)	SD or Range
Age (years)	40.1	6.1
Body mass index (kg/m^2)	27.5	4.7
Number of school years completed	17.3	3.5
Seated Resting SBP (mmHg)	120.3	9.4
Seated Resting DBP (mmHg)	72.6	9.2
Smoking Status		
Current	17.2%	
Former	22.6%	
Never	60.2%	
Measures of negative emotionality and life stress		
Depressive symptoms (BDI-II)	3.5	3.4
Anxiety symptoms (STAI-T)	32.9	7.8
Hostility (CMHS-total score)	14.9	7.4
Life stress (PSS)	1.3	0.6
Task accuracy (% correct)		
MSIT congruent condition (MRI replica)	93.3	3.6
MSIT incongruent condition (MRI replica)	56.1	5.8
MSIT congruent condition (MRI)	91.2	4.3
MSIT incongruent condition (MRI)	58.0	3.6
Task reaction time (ms)		
MSIT congruent condition (MRI replica)	516.1	105.6
MSIT incongruent condition (MRI replica)	844.0	193.7
MSIT congruent condition (MRI)	540.4	108.9
MSIT incongruent condition (MRI)	905.0	199.6
Change from baseline to MSIT in valence*		
MRI replica	-1.2	1.8
MRI	-1.1	1.6
Change from baseline to MSIT in arousal*		
MRI replica	2.6	2.3
MRI	2.3	2.1
Change from baseline to MSIT in control*		
MRI replica	-1.7	2.3
MRI	-1.3	2.5
Change from baseline to MSIT in BRS (ln-transform of ms/mmHg)*		
MRI replica	-0.1	0.2
Change from baseline to MSIT in SBP/DBP (mmHg)*		
MRI replica	6.5/3.8	7.8/4.6
MRI	4.8/1.5	6.2/4.5
Change from baseline to MSIT in HR (BPM)*		
MRI replica	3.7	4.0
MRI	6.8	5.3

Note. BDI-II = Beck Depression Inventory-II (1996, revised version); STAI-T = Spielberger State-Trait Anxiety Inventory-Trait version; CMHS = Cook-Medley Hostility Scale; PSS = Perceived Stress Scale. *Changes from baseline in valence, arousal, and control ratings, as well as BRS, BP, and HR changes were all statistically significant at Ps<0.005 by paired t-tests.

with an oscillometric device (Critikon Dinamap 8100, Johnson & Johnson, Tampa, FL) and taken 2 min apart after an ~20-min acclimation period.

All participants provided informed consent after receiving an explanation of study protocols. They were also tested in compliance with the Code of Ethics of the World Medical Association (Declaration of Helsinki), and with the approval of the University of Pittsburgh Institutional Review Board. Further descriptive information about participant characteristics are in Table I.

Study Protocols

Participants were tested in two separate study protocols in an experimental design comparable to that of fMRI studies of human baroreflex control under lower negative body pressure [Kimmerly et al., 2005]. One protocol involved continuous BP monitoring during the performance of a stressor task (see below) within a plastic MRI scanner replica; the other involved performance of the same task during fMRI (median intersession interval = 7

days, with fMRI testing occurring first across all subjects). Before both protocols, participants abstained from eating, exercising, and consuming caffeinated and tobacco products for 8 h and drinking alcoholic beverages for 12 h. Also, before the fMRI protocol, participants underwent a screening interview, followed by assessments of anthropometric measures, demographic information, psychosocial factors, and seated BP.

Stressor Task

Participants completed a task that evokes cardiovascular reactivity: a modified MSIT [Bush and Shin, 2006; Gianaros et al., 2009]. Subjective ratings of the task were obtained after performance (see below). The task lasted 9 min 20 s, and was comprised of two conditions: a *congruent* condition and an *incongruent* condition. The two conditions (52–60 s in length) were administered in a blocked design, and each was preceded by a variable 10–17 s period during which participants fixated on a crosshair. Briefly, the two conditions were matched on motor response requirements and visual stimulus characteristics. Further, the incongruent condition was performance-titrated, such that task accuracy was maintained below 60% on average within and between individuals by varying stimulus delivery times in a manner unpredictable to the participant. Task engagement and motor performance for both conditions were thus controlled across participants and testing sessions; incongruent and congruent conditions were also counterbalanced and presented four times each.

In both MSIT conditions, participants viewed three numbers in single trials; two numbers were identical, and one was different. Participants selected the different number by pressing one of three buttons on a response glove. For congruent trials, the target number was congruent with its spatial location on the response glove, such that the there was a one-to-one mapping between the target stimulus position and the position of the response option. For incongruent trials, the target number was incongruent with its location on the glove, such that there was an incongruent mapping between the target position and the response option. After each response, participants were given accuracy feedback (green $\surd$s and red *X*s). Additional MSIT details are reported in a study of a separate sample of participants [Gianaros et al., 2009].

Performance and Subjective Ratings

Task accuracy was computed as the percentage of trials completed correctly. We verified that mean accuracy during the incongruent condition was <60% across participants, and it was significantly worse compared with the congruent condition in the fMRI and replica testing sessions, $ts > 56.0$, $Ps < 0.001$ (Table I). Response times during the incongruent compared with the congruent condition were also slowed on both sessions, $ts > 30.2$, $P < 0.001$ (Table I).

To assess ratings of valence (1, very unhappy; 9, very happy), arousal (1, very calm; 9, very aroused), and perceived control (1, very little control; 9, very much control), participants completed a self-assessment manikin scale [Bradley and Lang, 1994] after the baseline (prestressor) and stressor task periods (Table I).

MRI Replica Protocol and BRS Assessment

We monitored beat-to-beat BP and interbeat intervals (IBIs; the time in ms between heart beats) while participants completed the MSIT inside of a plastic MRI replica (see above) to derive BRS estimates. (At present, beat-to-beat BP cannot be measured directly, safely, or without significant radiofrequency noise interference with existing commercial instrumentation in an fMRI environment [Gray et al., 2009a]). To the best of our ability, we attempted to match the replica protocol to the contextual characteristics of the fMRI protocol, facilitating an integration of cardiovascular and neuroimaging data across sessions (cf., Kimmerly et al., 2005; Wong et al., 2007]. Hence, the MRI replica had the same physical dimensions, color, and sliding table as the scanner used for fMRI; the postural position, birdcage head support, and stimulus presentation system also replicated those of the fMRI scanner. Behavioral responses were recorded with an identical response glove, controlled with same software implemented in the fMRI scanner. For the replica protocol, participants were placed on the "scanner bed" and fitted with an appropriately sized finger cuff for beat-to-beat BP monitoring using a Finometer® PRO (FMS, Finapres Measurement Systems, Arnhem, Netherlands). The cuff was applied on the hand unused for behavioral responding. Thereafter, an 8- to 10-min calibration period was implemented for stabilization of the finger BP waveform [Wesseling et al., 1995]. Beat-to-beat BP and IBIs were then recorded continuously for an 8-min prestressor baseline, followed by the stressor task. The participant's hand instrumented for BP monitoring rested just below the xiphisternal junction.

The Finometer® monitors arterial BP using a volume-clamp method. With an infrared photoplethysmograph, the device detects, digitally samples, and stores a reconstructed, continuous waveform of estimated brachial pressure. Here, finger arterial BP was (i) calibrated to brachial pressure using an upper-arm cuff provided with the Finometer® and a proprietary algorithm [Bogert and van Lieshout, 2005; Guelen et al., 2003], and it was (ii) corrected for the hydrostatic height of the finger with respect to heart level to compensate for the pressure gradient over the arteries of the arm [Gizdulich et al., 1996]. Digitized BP signals were visually inspected and scored offline using locally developed scripts and with BeatScope® software provided with the Finometer®.

BRS was computed using the *x*BRS software package, which uses a validated crosscorrelation, time-domain method to quantify "spontaneous" associations between

SBP and IBI values [La Rovere et al., 2008; Westerhof et al., 2004]. This method computes BRS by performing running crosscorrelations between SBP and IBI time-series in 10-s epochs using a delay ranging from 0 to 5 s and providing up to six correlations for each delay and epoch. For each epoch, the delay yielding (i) the highest correlation and (ii) a coefficient of determination significant at $P < 0.01$ was retained, and the respective regression slope was taken as the BRS estimate in ms/mmHg. If these conditions were unmet, a BRS estimate was not calculated. To reduce measurement error and allow for a sufficient number of sequences to be detected, providing for stable values comparable to those of other studies of stressor-evoked BRS suppression [Steptoe and Sawada, 1989], baseline BRS estimates were averaged over the last 5 min of the 8-min baseline, and task-related BRS estimates were averaged over the first 5 min of the task. As expected, BRS values were skewed [Westerhof et al., 2004] and were subjected to log-normal transformation. To compute the change in BRS (ΔBRS) as a measure of BRS reactivity, averaged baseline BRS values were subtracted from averaged task values.

fMRI Protocol and Data Acquisition

fMRI data were acquired while participants performed the MSIT within a 3 T Trio TIM whole-body MRI scanner (Siemens, Erlangen, Germany), equipped with a 12-channel phased-array head coil. Blood-oxygen level-dependent (BOLD) images were acquired over the task period with a gradient-echo EPI sequence using the following parameters: field-of-view (FOV) = 205 × 205 mm^2, matrix size = 64 × 64 mm^2, time-to-repetition (TR) = 2,000 ms, time-to-echo (TE) = 28 ms, and flip angle (FA) = 90°. Thirty-nine slices (3-mm thick, no gap) were obtained in an interleaved sequence in an inferior-to-superior direction, yielding 280 BOLD images (three initial discarded images, allowing for magnetic equilibration). For spatial coregistration of BOLD images, T_1-weighted 3D magnetization-prepared rapid gradient echo (MPRAGE) neuroanatomical images were acquired over 7 min 17 s by these parameters: FOV = 256 × 208 mm^2, matrix size = 256 × 208 mm^2, TR = 2,100 BOLD images were acquired over the task period with a gradient-echo EPI sequence by these parameters ms, time-to-inversion (TI) = 1,100 ms, TE = 3.29 ms, and FA = 8° (192 slices, 1-mm thick, no gap). During fMRI, BPs were taken intermittently using oscillometric methods employed in our prior studies [Gianaros et al., 2009]. Because detailed analyses of these BPs are beyond the scope of this study, they will be prepared fully for a companion report; summaries, however, are in Table I and available on request. Exploratory analyses of associations between BRS suppression and stressor-evoked BP reactivity are also provided below.

fMRI Data Preprocessing

fMRI data were preprocessed and analyzed with statistical parametric mapping software (SPM8; http://www.fil.ion.ucl.ac.uk/spm). Before analyses, BOLD images were realigned to the first image of the series by six-parameter rigid-body transformation. Realigned images were coregistered to each participant's T_1-weighted structural image. These coregistered images were normalized by 12-parameter affine transformation to the International Consortium for Brain Mapping 152 template (Montreal Neurological Institute; MNI). Finally, normalized images were smoothed with a 6-mm full-width-at-half-maximum (FWHM) Gaussian kernel.

Analysis of Covariation Between BRS and Regional Brain Activation

After preprocessing, a contrast image reflecting relative brain activation ("incongruent > congruent" BOLD signal change) was estimated for each participant. To this end, task conditions were modeled with rectangular waveforms convolved with the default SPM hemodynamic response function (HRF). Contrast images were then generated by general linear model (GLM) estimation. Before estimation, low-frequency BOLD signal noise was removed by high-pass filtering (187-s cut-off). Serial BOLD signal autocorrelations were also accounted for by a first-order autoregressive model. Finally, regression vectors derived from the realignment preprocessing step were included in the GLMs to account for BOLD signal changes attributable to head movement.

To determine the covariation between relative brain activation and the task-related change in BRS (ΔBRS) across participants according to our first hypothesis, contrast images (incongruent > congruent) were submitted to a regression model in SPM8. In the model, ΔBRS was entered as a covariate of interest. Age, sex, and baseline BRS were also entered as confounding covariates (Entering resting SBP to the model had no appreciable effects on the direction or statistical significance of any findings reported below; resting SBP was thus omitted for model parsimony). Given our primary focus on the cingulate cortex, insula, amygdala, and midbrain extending into the pons region of the brainstem, these areas were targeted in region-of-interest (ROI) analyses using anatomical masks detailed in Supporting Information Figure S1. For primary analyses, we used a corrected false-positive detection rate of 0.05 within the ROI volumes by employing voxel-wise and combined cluster extent thresholds that were empirically determined by the spatial smoothness of all statistical parametric maps and Monte Carlo simulations. Details regarding ROIs and procedures for determining statistical thresholds employed for primary analyses are in Supporting Information Figure S1. For completeness of reporting, we executed whole-brain and exploratory analyses of relative activation (incongruent > congruent) and relative deactivation ("congruent > incongruent"), the latter being operationally defined as fMRI BOLD signal changes that were comparatively *higher* during the congruent relative

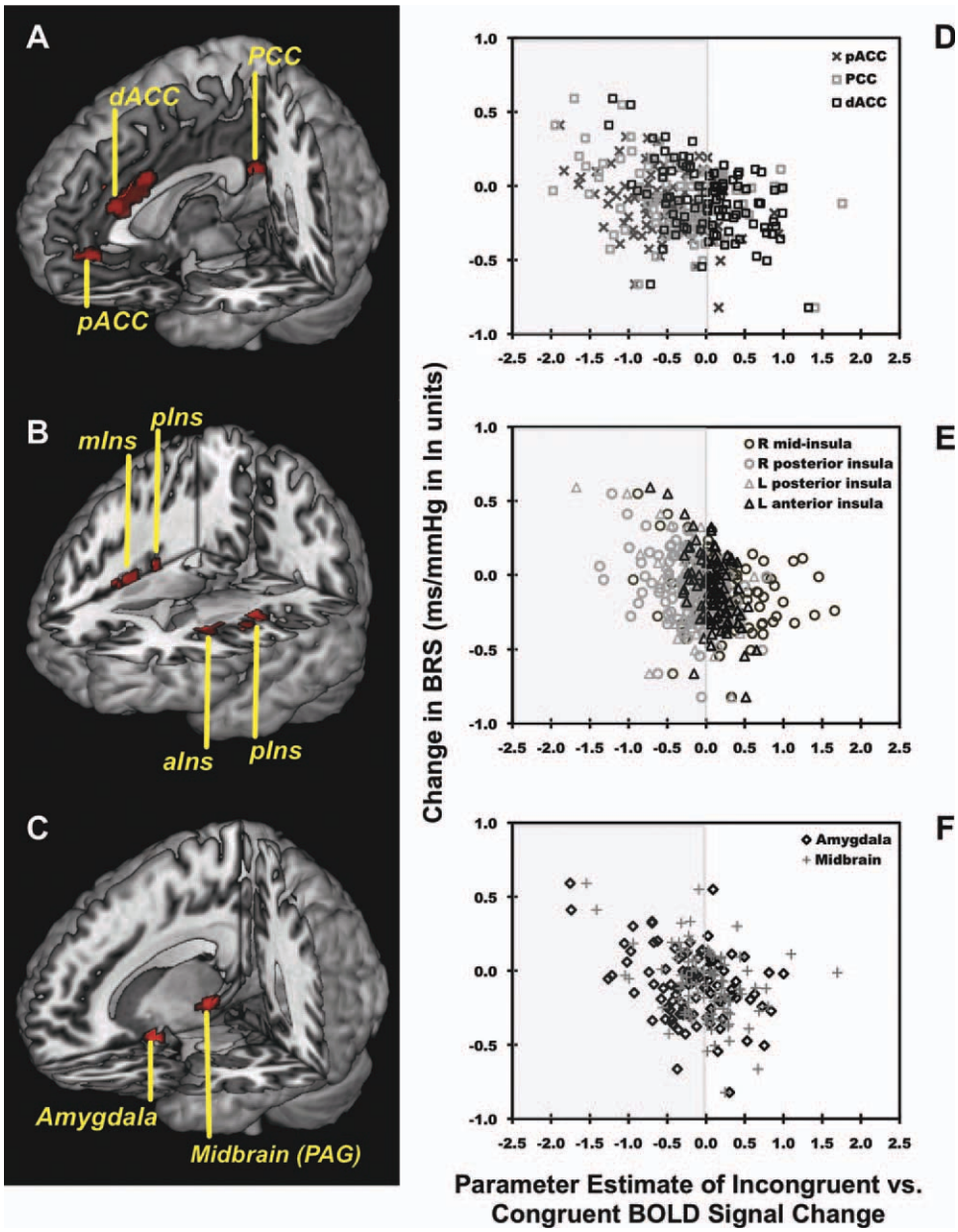

Figure 1.

Across 97 individuals, a greater suppression of BRS evoked by a MSIT covaried with higher relative levels of activity (incongruent > congruent condition BOLD signal changes) in the dACC, pCC, pACC, bilateral posterior insula (pIns), midinsula (mIns), and anterior insula (aIns), right amygdala, and right PAG. Profiled in (**A**–**C**) are areas of the dACC (*x*, *y*, and *z* coordinates for peak voxel in millimeter: 4, 28, and 24, $t_{92} = 4.9$, $P < 0.001$, voxel cluster size [*k*] = 380), pCC (−2, −44, 20, $t_{92} = 4.0$, $P < 0.001$, $k = 46$), pACC (0, 44, −4, $t_{92} = 4.0$, $P < 0.001$, $k = 48$), bilateral insula (right pIns: 42, −14, 6, $t_{92} = 4.6$, $P < 0.001$, $k = 323$; left pIns: −34, −12, 16, $t_{92} = 4.1$, $P < 0.001$, $k = 193$; left aIns: −30, 16, 14, $t_{92} = 4.8$, $P < 0.001$, $k = 57$; right mIns: 38, 10, 0, $t_{92} = 3.7$, $P < 0.001$, $k = 29$), right amygdala (20, −2, −22, $t_{92} = 4.4$, $P < 0.001$, $k = 50$), and PAG (14, −28, −4, $t_{92} = 4.1$, $P < 0.001$, $k = 32$) where higher BOLD activity levels covaried with a greater suppression of BRS, after controlling for age, gender, and resting BRS in a voxel-wise multiple regression model with multivariate control for voxel-wise statistical testing. Plots in (**D**–**F**) illustrate the change in BRS from baseline along the *y*-axis as a function of extracted parameter estimates of incongruent > congruent BOLD activity changes from the dACC, pCC, pACC, insula, amygdala, and midbrain plotted along the *x*-axis. Gray shading in the left panels of (D–F) encompass BOLD signal change values that corresponded to average relative decreases in BOLD activity during the incongruent compared with the congruent condition; white backgrounds to the right encompass values corresponding to average relative increases in activity during the incongruent compared with the congruent condition (see "Results" section). [Color figure can be viewed in the online issue, which is available at wileyonlinelibrary.com.]

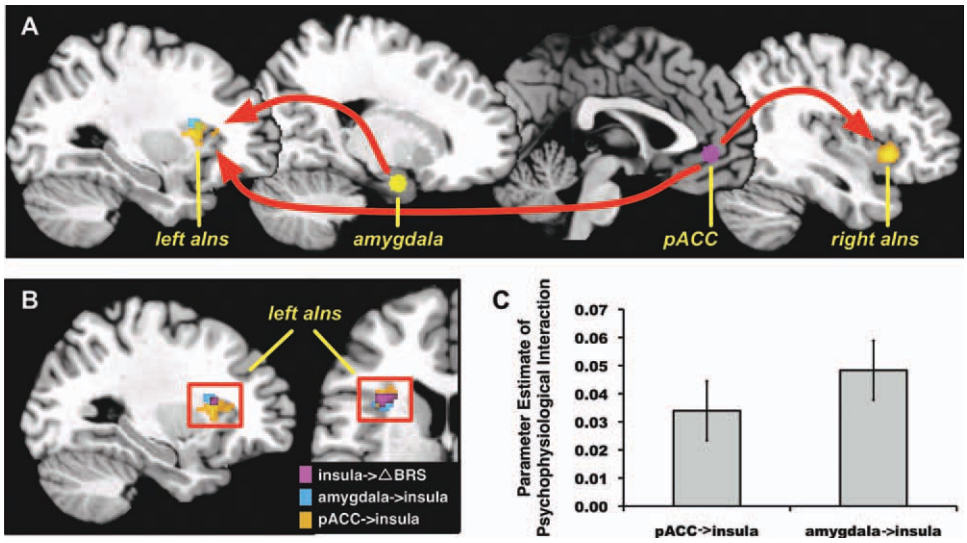

Figure 2.

During the incongruent condition of the MSIT, the pACC, and right amygdala exhibited an increase in the positive functional connectivity (time-varying covariation in BOLD signal activity) with a convergent region of the left anterior insula (aIns). Illustrated in (**A**) are the pACC and amygdala areas used as seed regions for PPI (connectivity) analyses (see "Methods" and "Results" sections). Also illustrated in (A) are regions of the insula where the pACC and amygdala exhibited increased functional connectivity. Illustrated in (**B**) is the region of the left anterior insula that expressed increased functional connectivity with the pACC and amygdala during incongruent condition of the MSIT stressor, as well as the portion of the anterior insula where a greater reduction in BRS from baseline to MSIT performance (ΔBRS) covaried with greater MSIT-related BOLD activation (as shown in Fig. 1). Illustrated in (**C**) are averaged, extracted functional connectivity values (parameter estimates of PPIs) for the pACC and left anterior insula and for the amygdala and left anterior insula. All analyses were executed with multivariate control for voxel-wise statistical testing (see "Methods" section and Supporting Information Figure S1). [Color figure can be viewed in the online issue, which is available at wileyonlinelibrary.com.]

to the incongruent task condition. We further executed whole-brain analyses of task-related changes in BRS and patterns of relative activation and deactivation at more lenient statistical thresholds for exploratory purposes and comparisons with future studies (see below).

Analysis of Functional Connectivity

Using psychophysiological interaction (PPI) analyses [Friston, 1994; Friston et al., 1997] to test our second hypothesis, we examined the degree to which the incongruent MSIT condition affected the temporal covariation (functional connectivity) of BOLD signal activity in the pACC and amygdala with activity in the insula. To test our third hypothesis, we examined the degree to which the incongruent MSIT condition affected the functional connectivity of the insula with the midbrain and pons. For PPI analyses, spatial neuroanatomical coordinates localized to the pACC, amygdala, and insula were treated as "seed" regions. Seed coordinates were selected on the basis of an *a priori* focus on the pACC, amygdala, and insula, as empirically constrained by (i) activation findings demonstrating that increased activity during the incongruent MSIT condition at these specific coordinates covaried significantly with ΔBRS across individuals (see "Results" section; Fig. 1) and (ii) connectivity findings demonstrating that during the incongruent MSIT condition, both the pACC and amygdala showed increased functional connectivity with a spatially overlapping area of the left anterior insula that also showed greater activation in association with ΔBRS (see "Results" section; Fig. 2).

For PPI analyses, we extracted a time-series representing the first eigenvariate of the BOLD signal for the pACC (x, y, and z coordinates in millimeters: 0, 44, and −4), right dorsal amygdala (20, −2, and −22), and left anterior insula (−30, 16, and 14) for each participant. Specifically, each time-series was extracted from the first principal component of BOLD signal activity in all voxels within a 6-mm radius surrounding the peak pACC, amygdala, and insula coordinates identified in the regression analyses relating ΔBRS to task-related activation (incongruent > congruent BOLD signal change). Next, each BOLD signal time-series was mean-centered and submitted to a deconvolution algorithm using the canonical SPM8 HRF. Following deconvolution, an interaction vector was created. This interaction vector represented the

product of the deconvolved BOLD signal time-series and a vector coding for task condition (incongruent > congruent). The interaction vector was subsequently re-convolved with the SPM8 HRF, creating a so-called PPI vector. Finally, all three vectors, corresponding to task condition, seed activity, and the PPI task-by-seed activity term, were entered as regressors in orthogonal individual GLM design matrices, wherein one PPI GLM was executed for each participant and seed region. Individual GLMs were then estimated, and contrasts were generated to test for statistically significant PPIs. Hence, individual GLMs testing for PPIs would demonstrate that interregional and time-dependent covariation (functional connectivity) with a given seed region was *greater* during the incongruent than congruent condition of the MSIT. As a result, PPI maps generated for each individual identified regions exhibiting *greater* functional connectivity with the pACC, amygdala, and insula in the incongruent as compared with the congruent condition.

Individual PPI maps were then entered into random-effects analyses, wherein condition-related effects (incongruent > congruent) on functional connectivity were tested in one-sample t-tests. In hypothesis-driven ROI analyses, we examined whether connectivity between the pACC and amygdala with the insula increased across individuals during the incongruent compared with the congruent condition using the same insula mask described above (Supporting Information Figure S1). To identify subcortical midbrain and pons regions exhibiting increased functional connectivity with the insula during the incongruent condition, we executed ROI analyses using the same midbrain and pons mask described above (Supporting Information Figure S1). For ROI PPI analyses, we maintained a corrected threshold of 0.05 within ROI volumes with empirically determined voxel-wise thresholds of $P < 0.001$, and cluster extent thresholds described in Supporting Information Figure S1. Finally, we executed whole-brain tests of pACC, amygdala, and insula connectivity at more lenient statistical thresholding for completeness of reporting and for comparison with future studies.

RESULTS

Stressor-Evoked Subjective Ratings and Cardiovascular Reactivity

The MSIT evoked subjective distress and an average reduction in BRS across participants. Specifically, using nine-point rating scales in both the replica and fMRI testing sessions, participants reported that they were less happy, more aroused, and less in control while performing the MSIT, as compared with the prestressor baseline period (*t*s for all task vs. baseline comparisons ≥ 5.2, $Ps \leq 0.001$; Table I). Participants also exhibited an average reduction in BRS from baseline ($M = 2.14$, SD = 0.44 ln-transformed units of ms/mm Hg) to the MSIT ($M = 2.04$, SD = 0.44; $t = 3.9$, $P < 0.001$), indicating an average suppression of BRS during task performance across participants.[1]

For illustrative purposes, average SBP, DBP, and HR time-series are shown as a function of MSIT conditions in Supporting Information Figure S2. As shown, the incongruent MSIT condition increased SBP, DBP, and HR compared with baseline, as well as the fixation and congruent periods during the fMRI replica testing session. Further, during fMRI testing, the incongruent condition evoked increases in these same cardiovascular parameters (Table I). These findings indicate collectively that the MSIT evoked subjective psychological distress and parallel changes in cardiovascular reactivity in both testing occasions.

Stressor-Evoked Covariation Between Regional Brain Activity and BRS

Across individuals, a *greater reduction* in BRS from baseline to the MSIT covaried with *greater relative activity* (incongruent > congruent BOLD signal change) in three areas of the cingulate cortex: the pACC, dorsal anterior cingulate cortex (dACC), and posterior cingulate cortex (pCC) (see Fig. 1). A greater stressor-evoked reduction in BRS also covaried with greater activity in the insula, amygdala, and midbrain PAG (see Fig. 1). Notably, these findings were obtained with multivariate control for voxel-wise statistical testing and covariate control for age, sex, and baseline BRS. Supporting Information Table S1 and Figure S3 list and illustrate areas revealed in whole-brain analyses and not of a priori focus, respectively, where greater stressor-evoked reductions in BRS covaried with greater incongruent > congruent BOLD activity.

There were no statistically significant associations between stressor-evoked changes in BRS and patterns of *greater relative deactivation* evoked by the MSIT, as reflected by BOLD signal changes that were *higher* during the congruent compared with the incongruent condition (quantified by the congruent > incongruent contrast). This null finding was not due to the fact that the MSIT did not evoke significant relative deactivation patterns. Hence, whole-brain analyses revealed patterns of both relative activation (incongruent > congruent BOLD signal changes) and relative deactivation (congruent > incongruent BOLD signal changes). More precisely, random-effects analyses of the incongruent > congruent condition contrast revealed relative *activation* in brain regions likely supporting functions engaged by the incongruent condition, including executive control, working memory, conflict and error monitoring, response inhibition, and other cognitive and

[1] Men and women did not differ in task ratings. Nor did they differ in BRS changes from baseline to the MSIT, $Ps > 0.05$ by *t*-tests. Given these null findings, results are presented for men and women combined. For consistency, however, sex was retained as an a priori covariate in all analyses as planned. Additionally, accuracy, response times, and valance, arousal, and control ratings did not show significant univariate correlations with the change in BRS from baseline to task, all $Ps > 0.29$.

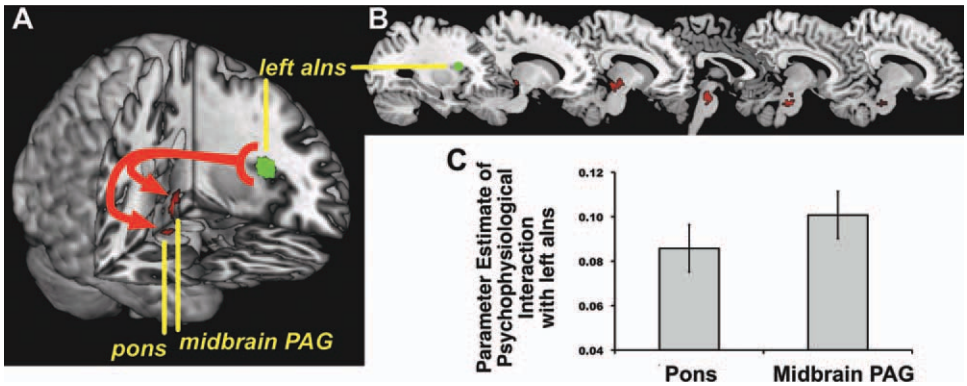

Figure 3.

During the incongruent condition of the MSIT, the left anterior insula (left aIns) exhibited an increase in positive functional connectivity with the pons and midbrain PAG. Illustrated in (**A**) is the left anterior insula area used as a seed region for PPI (connectivity) analyses (see "Methods" and "Results" section), along with pons and midbrain PAG regions showing increased insula connectivity. The left aIns region was chosen as a seed region because it showed increased activation in association with a suppression of BRS and because it expressed increased functional connectivity with the pACC and right amygdala during the incongruent task condition. Illustrated in (**B**) are successive sagittal slices showing the extent of pons and midbrain PAG regions expressing increased functional connectivity with the left aIns during incongruent condition of the task. Illustrated in (**C**) are averaged, extracted insula functional connectivity values (parameter estimates of PPIs) for the pons and midbrain PAG. All analyses were executed with multivariate control for voxel-wise statistical testing (see "Methods" section and Supporting Information Figure S1). [Color figure can be viewed in the online issue, which is available at wileyonlinelibrary.com.]

salience appraisal functions supporting time-pressured and accurate responding. These regions included the dACC, anterior insula, dorsolateral prefrontal cortex, parietal lobe, thalamus, cerebellum, and others illustrated in Supporting Information Figure S4 and listed in Supporting Information Table S2. In parallel, random-effects analyses of the congruent > incongruent condition contrast revealed *relative deactivation* patterns in brain regions that reliably show high levels of metabolic activity and functional connectivity during resting or minimally demanding behavioral states. These regions are viewed to comprise a "default mode network" that are also thought to be partly involved in visceral homeostatic and autonomic control functions, and here included the perigenual and pCC, amygdala, posterior insula and other regions detailed in Supporting Information Figure S4 and Table S2 [Buckner et al., 2008; Greicius et al., 2003; Kimmerly et al., 2005; Nagai et al., 2004; Wong et al., 2007].

In view of the above, the inverse covariation between ΔBRS and BOLD signal changes in the perigenual and posterior cingulate, amygdala, and posterior insula regions indicates that higher activity levels or *lesser relative deactivation* in these regions associates with a greater suppression of BRS across individuals (see Fig. 1). In extension, the inverse covariation between ΔBRS and BOLD signal changes in the dACC and anterior insula indicate that higher activity levels or *greater relative activation* in these regions associates with a greater suppression of BRS (see Fig. 1).

Functional Connectivity of the pACC and Amygdala With the Insula

The incongruent MSIT condition increased the positive functional connectivity of the pACC and amygdala with a spatially convergent area of the left anterior insula (see Fig. 2). Critically, and as detailed above, this same anterior insula area also exhibited increased activation (incongruent > congruent BOLD signal change) in association with a greater stressor-evoked suppression of BRS. Further, the pACC, but not amygdala, exhibited increased positive functional connectivity with the right anterior insula during the incongruent condition. Altogether, these findings reflect (i) a lateralized pattern of convergent positive functional connectivity between the pACC and amygdala with the left anterior insula, and (ii) a bilateral pattern of positive functional connectivity between the pACC and right and left anterior insula. Supporting Information Table S3, and Figures S5 and S6 provide complete listings and illustrations of other regions revealed in whole-brain analyses where the pACC and amygdala exhibited increased positive functional connectivity during the incongruent MSIT condition.

Functional Connectivity of the Insula With Midbrain and Pons

During the incongruent MSIT condition, the left anterior insula, specifically the area where greater activation

covaried with a greater stressor-evoked BRS suppression and where increased functional connectivity was exhibited with the pACC and amygdala, showed an increase in positive functional connectivity with the midbrain PAG and brainstem pons (see Fig. 3). Supporting Information Figure S7 and Table S3 provide complete listings and illustrations of other regions identified in whole-brain, exploratory analyses where the left anterior insula exhibited increased positive functional connectivity during the incongruent MSIT condition.

DISCUSSION

This study provides three lines of new human evidence that individual differences in the stressor-evoked suppression of the baroreflex covary with the functional activity and network properties of brain systems previously implicated in the integration of contextually adaptive behavior and autonomic cardiovascular control. First, a greater reduction in BRS to a cognitive or psychological stressor (MSIT) covaried across 97 individuals with patterns of greater relative activation and lesser relative deactivation within areas of the cingulate cortex, amygdala, and insula that have been implicated specifically in stressor-evoked BP reactivity [Gianaros and Sheu, 2009]. Second, during stressor processing, the functional connectivity of the amygdala and the pACC increased with a spatially convergent area of the left anterior insula. And third, during stressor processing, this same left anterior insula area that exhibited (i) increased functional connectivity with the pACC and amygdala and (ii) increased activation in association with reduced BRS also exhibited (iii) increased functional connectivity with midbrain PAG and pons areas that are considered as supra-medullary cell groups involved in baroreflex regulation. Together, these lines of evidence extend prior work by characterizing the brain systems by which psychological stressors can affect cardiovascular reactivity through a baroreflex pathway.

Psychological stress is considered as a poorly understood biobehavioral risk factor for essential hypertension and atherosclerotic cardiovascular disease [Brotman et al., 2007]. A particular stress-related factor that is widely implicated in cardiovascular disease risk is an individual's tendency to show exaggerated cardiovascular reactions to acute psychological stressors, particularly cognitive stressors that are standardized in a manner matching the experimental characteristics of the stressor employed here [Chida and Steptoe, 2010; Kamarck and Lovallo, 2003; Treiber et al., 2003]. Yet in contrast to appreciable epidemiological evidence on stressor-evoked cardiovascular reactivity and disease risk [Chida and Steptoe, 2010], there is little evidence for the mechanistic neurobiological pathways that link the central nervous system processing of psychological stressors with the peripheral expression of cardiovascular reactions implicated in cardiovascular pathophysiology [Lane et al., 2009b]. A recent meta-analysis [Gianaros and Sheu, 2009] of the existing neuroimaging literature in this area identified three particular regions that appear to play key functions in mediating individual differences in stressor-evoked cardiovascular reactivity, including areas of the cingulate, amygdala, and insula, as well as several other networked cortical and subcortical areas involved in mobilizing hemodynamic and metabolic support for adaptive behavioral responding. A working neurobiological model developed in this meta-analytic review led to the prediction that the functionality of these regions in humans should be associated not only with stressor-evoked changes in BP and HR but also changes in the sensitivity of the baroreflex that enable end organ activity changes at the level of the myocardium and vasculature [see Fig. 1 in Gianaros and Sheu, 2009]. To our knowledge, this study provides the first support for this prediction.

To elaborate, a key pathway through which the processing of psychological stressors can generate and regulate acute cardiovascular reactions is via descending central nervous system influences over the baroreflex [Berntson et al., 1998; Dampney, 1994]. Hence, during stressor processing, regions of the cingulate, amygdala and insula can suppress the sensitivity of the baroreflex via anatomical projections that (i) inhibit activity in parasympathetic source nuclei and (ii) activate sympathetic source nuclei, allowing BP and HR to rise simultaneously [Berntson et al., 1998; Dampney, 1994]. In addition to these efferent (or descending) control mechanisms, these same brain regions can be modulated by interoceptive visceral afferent (or ascending) influences of baroreflex activity [Berntson et al., 1998; Cechetto and Shoemaker, 2009; Dampney, 1994; Gianaros and Sheu, 2009]. Hence, the primary brainstem region instrumental for relaying visceral afferent information, particularly baroreceptor information, to higher brain regions is the NTS [Berntson et al., 2003; Dampney, 1994; Guyenet, 2006]. From the NTS, poly-synaptic projections are issued not only to medullary and preautonomic brainstem, pontine, and midbrain cell groups but also via thalamus to cingulate cortex (particularly the perigenual portion), amygdala, and insula [Allen and Cechetto, 1992, 1993; Allen et al., 1991; Berntson et al., 2003; Buchanan and Powell, 1993; Dampney, 1994; Dampney et al., 2002, 2003]. Thus viewed as integrated components of parallel feedforward and feedback control circuits, areas of the cingulate, amygdala, and insula may provide for an interface between stressor processing and the integration and afferent representation of visceral information regarding acute stressor-evoked cardiovascular changes - particularly in the service of preparing for and enabling contextually adaptive and motivated behavioral action (e.g., "approach vs. avoidance" or "fight vs. flight" coping behaviors) [Dampney, 1994; Dampney et al., 2002]. For instance, baroafferent signaling resulting from stressor-evoked increases in BP may be relayed via the NTS for representation by forebrain regions, including regions of the cingulate, amygdala, and insula. This stressor-evoked visceral afferent information may then

modulate ongoing activity these regions in a positive or negative feedback manner, which could further modulate descending signaling with midbrain and brainstem circuits, including the PAG and pons. This modulated signaling resulting from ascending visceral feedback could serve to adjust cardiovascular functioning-which, in aggregate, could impact the magnitude of stressor-evoked cardiovascular changes. In agreement with this conjecture, it is noteworthy that the stressor-evoked change in SBP assessed during the fMRI protocol (Table I) covaried inversely across individuals with BRS assessed during MSIT performance in the fMRI replica protocol, meaning that a greater suppression of the baroreflex predicted larger rises in stressor-evoked BP ($r = -0.23$, $P < 0.05$). Such findings would further appear to support the notion that human central autonomic control mechanisms are under the regulation of higher-order or supra-medullary brain systems, and that dysregulated activity in these systems associates with patterns of peripheral physiology prospectively associated with cardiovascular disease risk [Gianaros et al., 2008; Mujica-Parodi et al., 2009].

A notable limitation of this study, however, is that while patterns of relative activation and deactivation within the cingulate, amygdala, insula and other regions listed in Supporting Information Table S1 covaried with stressor-evoked changes in BRS across individuals, it is unclear whether these patterns of covariation reflected efferent, afferent, or both kinds of central autonomic cardiovascular control functions. Hence, we are pursuing the use of methods that integrate continuous BP monitoring and simultaneous neuroimaging to provide for the temporal resolution needed to resolve the issue of whether BP changes *precede* or *follow* changes in fMRI BOLD activity, as has been attempted in recent work [Cechetto and Shoemaker, 2009; Gray et al., 2009b]. This will permit a more formal test of whether baroreflex suppression concurrently explains (mediates) the magnitude of BP rises during psychological stress.

Functional connectivity findings also provided evidence that the anterior insula is apparently important for integrating inputs from the anterior cingulate and amygdala during stressor-processing, particularly in association with stressor-evoked baroreflex suppression. The anterior insula expresses dense reciprocal connections with the anterior cingulate, amygdala, and other regions that control autonomic source nuclei that regulate peripheral target organs, including those in the midbrain PAG, pons, and medullary areas [Augustine, 1996; Cechetto, 1994; Öngür and Price, 2000; Verberne and Owens, 1998]. Further, afferent relays from all target organs project to the insula along a caudal-to-rostral extent. These projections are routed via the NTS, parabrachial pons nuclei, thalamus, and hypothalamus, and they provide the insula with a "viscerotopic" map of the body [Craig, 2003; Harrison et al., 2010]. Such a map may support the integration of interoceptive information with the appraisal of salient environmental stimuli and contextually adaptive behavioral and autonomic responses [Cauda et al., 2011; Critchley, 2005; Greicius et al., 2003]. Further, lesion, stimulation, neuroanatomical tracing, and *in vivo* brain imaging evidence strongly implicates the insula in autonomic and cardiovascular control, particularly via efferent and modulatory afferent sympathetic, parasympathetic, and baroreflex pathways [Allen et al., 1991; Cechetto, 1994; Cechetto and Chen, 1990; Oppenheimer, 1993; Ruggiero et al., 1987; Verberne and Owens, 1998; Yasui et al., 1991]. Across prior human and animal studies, there is some, albeit mixed, evidence that the insular control of autonomic and cardiovascular function may be lateralized, with the left insula being more involved in parasympathetic control and the right insula in sympathetic control [Craig, 2005; Kimmerly et al., 2005; Oppenheimer et al., 1992, 1996; Thayer and Lane, 2009]. Further, spontaneous BRS measures, as used here, show appreciable covariation with indicators of cardiac parasympathetic control, such as indicators of high-frequency HR variability [Thayer et al., 2010]. In this regard, it is noteworthy in some respects that the pACC and amygdala exhibited increased positive functional connectivity with a convergent zone of the left anterior insula during stressor processing, and that greater activation of this same left anterior insula area covaried with a greater suppression of BRS (Figs. 1 and 2). Hence, a possible interpretation of these activation and connectivity findings is that this presumptive convergence zone of the left anterior insula may have supported integrative stressor-evoked autonomic, possibly parasympathetic, cardiovascular control changes in the context of the present MSIT paradigm. However, not all evidence is consistent with generalizations regarding lateralized autonomic cardiovascular control [e.g., Nagai et al., 2010]. For instance, Ahern et al. [2001] demonstrated that inactivation of the right hemisphere by the Wada test in epilepsy patients resulted in a greater suppression of parasympathetic cardiac control and a greater cardioaccelerative response than did left-hemispheric inactivation, suggesting a greater right-sided cortical control over parasympathetic activity. Evidence for asymmetrical insular control over BP is similarly mixed. For example, bilateral [Gianaros et al., 2005, 2008] and left unilateral [Gianaros et al., 2007] insular activation patterns have been associated with BP reactivity evoked by a Stroop color-word interference cognitive stressor. Also, there is recent evidence that heightened levels of resting neural activity in the right insula prospectively predict greater stressor-evoked BP reactions across individuals, possibly reflecting an individual's "preparedness" to exhibit heightened pressor reactivity [Gianaros et al., 2009]. Further, non-invasive estimates of baroreflex activity are multiply and complexly determined by both sympathetic and parasympathetic nervous system influences, as well as respiratory mechanisms that we were unable to assess in the present study [Cohen and Taylor, 2002; La Rovere et al., 2008]. Finally, we note that baroreflex suppression in the present study was associated with elevated stressor-evoked activity in both the left *and* right anterior and caudal insula (see Fig. 1). Hence, the

relative inconsistency of existing literature and our prior findings hinders precise conclusions regarding a potential lateralized insular regulation of stressor-evoked BP reactivity via specific autonomic pathways. Nonetheless, it is clear from both human and animal work and the present findings that the insula is functionally associated with stressor-evoked cardiovascular changes, presumptively via efferent and afferent signaling with networked cortical and subcortical areas important for autonomic and physiological control [Cechetto and Shoemaker, 2009].

The present findings also extend prior work on anterior cingulate functionality in association with measures of behaviorally evoked *cardiac autonomic* and *cardiovascular* reactivity [Ahs et al., 2009; Critchley et al., 2003; Gianaros et al., 2004; Kimmerly et al., 2005; Lane et al., 2009a; Wager et al., 2009a,b; Wong et al., 2007]. Anatomically, regional differences in receptor expression, cellular architecture, and anatomical projections to and from other brain regions have long been held to define two broad and interacting subdivisions of the anterior cingulate that both appear to be important for stressor information processing and stressor-evoked physiological reactivity, which are nominally labeled as (i) a rostral or perigenual area (pACC) and (ii) a dorsal or supragenual area (dACC) [Bush et al., 2000; Devinsky et al., 1995; Palomero-Gallagher et al., 2008; Paus, 2001; Vogt, 2005; Vogt et al., 1992, 1995]. Hence, in addition to supporting a range of cognitive- and emotion-related functions, cumulative evidence implicates each of these anterior cingulate areas in association with stressor-evoked cardiovascular reactivity. In particular, the pACC has been viewed to support the experience of emotional states and the regulation of behavioral and autonomic responses to emotional stimuli [Bush et al., 2000; Critchley, 2005; Etkin et al., 2011; Lane et al., 2009b; Paus, 2001; Phillips et al., 2003; Vogt, 2005]. Animal and human findings further document a role for the pACC in stressor-evoked autonomic and cardiovascular reactivity, as instantiated through its dense and direct reciprocal circuitry with areas of the orbitomedial prefrontal cortex, anterior insula, amygdala, hypothalamus, PAG, pons, and medulla [Barbas, 2000; Barbas et al., 2003; Buchanan and Powell, 1993; Chiba et al., 2001; Critchley, 2005; Freedman et al., 2000; Vogt, 2005]. In recent imaging work, individual differences in stressor-evoked pACC activity have been associated specifically with greater stressor-evoked HR [Wager et al., 2009a,b] and BP reactivity [Gianaros et al., 2005, 2007, 2008].

Regions within the dACC are broadly viewed to support the emotional appraisal of behaviorally salient stimuli, attention, effortful executive control, and conflict and error monitoring, as instantiated by reciprocal circuitry with the lateral prefrontal cortex (areas 9/46), motor and supplementary motor cortex (areas 4/6), and posterior parietal cortex (area 7) [Vogt and Pandya, 1987]. A conventional view is that dACC areas are particularly important for monitoring conflicts between competing streams of incompatible information, which foster the potential for behavioral error [Botvinick et al., 2001; Hester et al., 2004; Holroyd and Coles, 2002; Ridderinkhof et al., 2004a,b]. After conflict detection, dACC areas engage prefrontal, motor, and parietal cortices to resolve conflicts and minimize behavioral error by modulating attention, working memory, and motor control processes [Koski and Paus, 2000; Paus, 2001; Paus et al., 1998]. Compatible with these notions, the MSIT task used in the present study robustly engaged the dACC across participants (Supporting Information Table S2 and Figure S4). Moreover, growing evidence further implicates dACC areas in emotional appraisal processes associated with physiological reactivity and subjective distress [Eisenberger and Lieberman, 2004; Etkin et al., 2011]. For example, dACC areas are engaged by the intentional regulation of autonomic activity [Critchley et al., 2001, 2002] and awareness of subjective emotional experiences [Lane et al., 1998]. Critchley [2005] has further posited that the dACC may be particularly important for generating autonomic and cardiovascular responses to support effortful cognitive and emotional behaviors. Consistent with this view, stressor-evoked BP reactivity has been shown to covary with heightened dACC activation [Gianaros et al., 2005]. And extending prior observations, greater activation in the dACC to the MSIT in the present study was shown to covary with a greater suppression of BRS across individuals (see Fig. 1). Interestingly, exploratory PPI connectivity analyses using the dACC region illustrated in Figure 1 as a seed region showed that in the incongruent condition of the MSIT, dACC connectivity increased positively with several regions of the prefrontal cortex (bilateral dorsolateral prefrontal cortex [BA46]; right orbitofrontal cortex [BA11]; dorsal medial prefrontal cortex [BA9]; rostral anterior cingulate [BA32]), as well as with the inferior parietal cortex [BA40] and right insula [BA13] (Supporting Information Figure S8). These patterns of task-modulated connectivity are consistent with previously reported patterns of dACC connectivity observed in other behaviorally aversive task paradigms (e.g., those involving fear conditioning or the processing of emotional conflict [see Fig. 2 in Etkin et al., 2011]. Hence, it may be possible to interpret our findings by the conceptual view that a critical and integrative role of the dACC, particularly during effortful cognitive tasks, involves the generation, representation, and control of autonomic activity patterns that are integrated with contextually appropriate and adaptive behaviors [Critchley, 2005; Etkin et al., 2011].

Finally, lesser relative deactivation of the pCC, a canonical hub of the default mode network [Buckner et al., 2008; Greicius et al., 2003; Seeley et al., 2007], was also found to covary with a greater stressor-evoked suppression of BRS (see Fig. 1). Functional changes within the pCC have been observed in association with several measures of autonomic cardiovascular activity [e.g., Gianaros and Sheu, 2009; Kimmerly et al., 2005; O'Connor et al., 2007; Wong et al., 2007]; however, the meaning of these functional changes presently lack a consensus of interpretation. This

is because the pCC does *not* express direct or dense connections with preautonomic control areas, as compared with anterior cingulate regions [Gianaros and Sheu, 2009; Vogt and Laureys, 2005]. Hence, in view of existing evidence, known neuroanatomical connections of the pCC, and established functions of the default mode network, it has been hypothesized that greater activity (or lesser relative deactivation) in this region during stressful or effortful cognitive tasks may correspond to a decreased capacity to curtail self-referential (default mode) processing or to a heightened evaluative appraisal of self-relevant and behaviorally salient information. Such activity may in turn indirectly (or even spuriously) relate to autonomic and cardiovascular changes because of *concurrent* changes in the activity of cortical and subcortical areas (e.g., ACC, amygdalar, and insular areas) that do project to preautonomic autonomic cell groups involved in cardiovascular control [Gianaros and Sheu, 2009; Wong et al., 2007].

To close, it is important to weigh the inferential points discussed above on balance with key methodological constraints of the present study. First, individual differences in baroreflex functionality were assessed while participants performed the MSIT in a replica or "mock fMRI" paradigm. These individual differences in baroreflex activity were then correlated to regional brain activity patterns assessed while participants performed the MSIT during fMRI. Hence, we did not evaluate *concurrently* measured individual differences in baroreflex functionality and regional brain activity. Hence, future methodological advances that enable the concurrent measurement of functional brain activity and continuous (beat-to-beat) cardiovascular activity to derive estimates of baroreflex activity should be exploited in order to replicate the present observations [Gray et al., 2009a]. Second, we attempted to match the replica protocol on salient contextual characteristics of the fMRI protocol to better facilitate the integration of cardiovascular and neuroimaging data across the two sessions [cf., Kimmerly et al., 2005; Wong et al., 2007]. In this regard, the MRI replica had the same confining dimensions, color, and sliding table as the scanner used for fMRI testing. The experimental instructions, postural position, caged head support, and stimulus presentation and response recording systems were also the same as those used for the fMRI testing session. Some important testing features, however, differed. For example, we were unable to generate the same background or ambient gradient noise in the replica testing session as is characteristic of fMRI testing. During replica testing, participants were also aware of the fact that they were not inside of an actual MRI, and they completed this testing session on a separate day following fMRI testing. In this regard, it is possible that such limitations could have differentially impacted the participants' cardiovascular reactivity, subjective task appraisals, and behavioral performance between testing contexts. We note, however, that subjective task ratings and performance metrics were correlated across the two sessions. For example, individual differences in subjective ratings of arousal, control, and valence summarized in Table I all correlated at 0.70 or higher across the testing contexts (all $Ps < 0.001$). Further, because we used a performance-titration procedure in an attempt to experimentally control for potential task engagement (or cognitive stressor intensity) differences within and across participants and testing sessions, we observed moderately high correlations across sessions in the number of MSIT trials completed ($r = 0.86$, $P < 0.001$) and in average reaction times ($r = 0.85$, $P < 0.001$). We further note that our MSIT testing protocol is modeled after cognitive stressor paradigms used in the cardiovascular behavioral medicine literature that are designed explicitly to evoke reliable (stable) differences in autonomic and cardiovascular reactivity over multiple testing sessions [Kamarck et al., 1992; Kamarck and Lovallo, 2003]. Consistent with this modeling, we observed moderate agreement in BP and HR reactivity values (computed as changes from baseline to the incongruent MSIT condition) across subjects, with rs ranging from 0.50 to 0.71, Ps < 0.001. Third, the order of the two testing sessions was fixed across participants, with fMRI testing occurring first. Finally, we did not use the same cardiovascular monitoring instrumentation in both sessions (e.g., intermittent oscillometric brachial artery monitoring during MRI and continuous finger volume-clam monitoring during replica testing), which would permit formal comparisons and tests for possible MSIT repetition effects on cardiovascular reactions across the two testing contexts. Thus, the interpretations above should be taken as provisional in consideration of these limitations.

CONCLUSION

The present findings provide novel human evidence for the brain systems presumptively involved in regulating baroreflex physiology during psychological stress. The present findings also provide further evidence that these brain systems should not only be viewed as canonical components of so-called cognitive-control and default-mode networks but also networks important for jointly processing salient environmental information and contextually regulating autonomic and cardiovascular activity in parallel with adaptive behavioral action (cf. Seeley et al., 2007]. Future work should determine the clinical relevance of these findings by testing whether stressor-evoked changes in the functionality of these brain systems associate with risk for essential hypertension and atherosclerotic heart disease endpoints already associated with and baroreflex impairments [La Rovere et al., 2008].

ACKNOWLEDGMENTS

The authors thank Sara Snyder for her assistance in data collection and project management.

REFERENCES

Ahern GL, Sollers JJ, Lane RD, Labiner DM, Herring AM, Weinand ME, Hutzler R, Thayer JF (2001): Heart rate and heart rate variability changes in the intracarotid sodium amobarbital test. Epilepsia 42:912–921.

Ahs F, Sollers JJ III, Furmark T, Fredrikson M, Thayer JF (2009): High-frequency heart rate variability and cortico-striatal activity in men and women with social phobia. NeuroImage 47:815–820.

Allen GV, Cechetto DF (1992): Functional and anatomical organization of cardiovascular pressor and depressor sites in the lateral hypothalamic area. I. Descending projections. J Comp Neurol 315:313–332.

Allen GV, Cechetto DF (1993): Functional and anatomical organization of cardiovascular pressor and depressor sites in the lateral hypothalamic area. II. Ascending projections. J Comp Neurol 330:421–438.

Allen GV, Saper CB, Hurley KM, Cechetto DF (1991): Organization of visceral and limbic connections in the insular cortex of the rat. J Comp Neurol 311:1–16.

Augustine JR (1996): Circuitry and functional aspects of the insular lobe in primates including humans. Brain Res Rev 22:229–244.

Barbas H (2000): Connections underlying the synthesis of cognition, memory, and emotion in primate prefrontal cortices. Brain Res Bull 52:319–330.

Barbas H, Saha S, Rempel-Clower N, Ghashghaei T (2003): Serial pathways from primate prefrontal cortex to autonomic areas may influence emotional expression. BMC Neurosci 4:25.

Barefoot JC, Dodge KA, Peterson BL, Dahlstrom WG, Williams RB Jr (1989): The Cook-Medley hostility scale: Item content and ability to predict survival. Psychosom Med 51:46–57.

Beck AT, Steer RA, Ball R, Ranieri W (1996): Comparison of Beck Depression Inventories-IA and -II in psychiatric outpatients. J Personal Assess 67:588–597.

Berntson GG, Sarter M, Cacioppo JT (1998): Anxiety and cardiovascular reactivity: The basal forebrain cholinergic link. Behav Brain Res 94:225–248.

Berntson GG, Sarter M, Cacioppo JT (2003): Ascending visceral regulation of cortical affective information processing. Eur J Neurosci 18:2103–2109.

Berntson GG, Norman GJ, Bechara A, Bruss J, Tranel D, Cacioppo JT (2011): The insula and evaluative processes. Psychol Sci 22:80–86.

Bogert LW, van Lieshout JJ (2005): Non-invasive pulsatile arterial pressure and stroke volume changes from the human finger. Exp Physiol 90:437–446.

Botvinick MM, Braver TS, Barch DM, Carter CS, Cohen JD (2001): Conflict monitoring and cognitive control. Psychol Rev 108:624–652.

Bradley MM, Lang PJ (1994): Measuring emotion: The self-assessment manikin and the semantic differential. J Behav Ther Exp Psychiatry 25:49–59.

Brotman DJ, Golden SH, Wittstein IS (2007): The cardiovascular toll of stress. Lancet 370:1089–1100.

Buchanan SL, Powell DA (1993): Cingulothalamic and prefrontal control of autonomic function. In: Vogt BA, Gabriel M, editors. Neurobiology of the Cingulate Cortex and Limbic Thalamus: A Comprehensive Handbook. Boston: Birkhauser. pp 381–414.

Buckner RL, Andrews-Hanna JR, Schacter DL (2008): The brain's default network: Anatomy, function, and relevance to disease. Ann NY Acad Sci 1124:1–38.

Bush G, Shin LM (2006): The Multi-Source Interference Task: An fMRI task that reliably activates the cingulo-frontal-parietal cognitive/attention network. Nat Protocol 1:308–313.

Bush G, Luu P, Posner MI (2000): Cognitive and emotional influences in anterior cingulate cortex. Trends Cog Sci 4:215–222.

Cauda F, D'Agata F, Sacco K, Duca S, Geminiani G, Vercelli A (2011): Functional connectivity of the insula in the resting brain. NeuroImage 55:8–23.

Cechetto DF (1994): Identification of a cortical site for stress-induced cardiovascular dysfunction. Integr Physiol Behav Sci 29:362–373.

Cechetto DF, Chen SJ (1990): Subcortical sites mediating sympathetic responses from insular cortex in rats. Am J Physiol 258:R245–R255.

Cechetto DF, Shoemaker JK (2009): Functional neuroanatomy of autonomic regulation. Neuroimage 47:795–803.

Chiba T, Kayahara T, Nakano K (2001): Efferent projections of infralimbic and prelimbic areas of the medial prefrontal cortex in the Japanese monkey, *Macaca fuscata*. Brain Res 888:83–101.

Chida Y, Steptoe A (2010): Greater cardiovascular responses to laboratory mental stress are associated with poor subsequent cardiovascular risk status: A meta-analysis of prospective evidence. Hypertension 55:1026–1032.

Cohen MA, Taylor JA (2002): Short-term cardiovascular oscillations in man: Measuring and modelling the physiologies. J Physiol 542:669–683.

Cohen S, Kamarck T, Mermelstein R (1983): A global measure of perceived stress. J Health Soc Behav 24:385–396.

Cook WW, Medley DM (1954): Proposed hostility and pharisaic-virtue scales for the MMPI. J Appl Psychol 38:414–418.

Craig AD (2003): Interoception: The sense of the physiological condition of the body. Curr Opin Neurobiol 13:500–505.

Craig AD (2005): Forebrain emotional asymmetry: A neuroanatomical basis? Trends Cogn Sci 9:566–571.

Critchley HD (2005): Neural mechanisms of autonomic, affective, and cognitive integration. J Comp Neurol 493:154–166.

Critchley HD, Melmed RN, Featherstone E, Mathias CJ, Dolan RJ (2001): Brain activity during biofeedback relaxation: A functional neuroimaging investigation. Brain 124:1003–1012.

Critchley HD, Melmed RN, Featherstone E, Mathias CJ, Dolan RJ (2002): Volitional control of autonomic arousal: A functional magnetic resonance study. NeuroImage 16:909–919.

Critchley HD, Mathias CJ, Josephs O, O'Doherty J, Zanini S, Dewar BK, Cipolotti L, Shallice T, Dolan RJ (2003): Human cingulate cortex and autonomic control: Converging neuroimaging and clinical evidence. Brain 126:2139–2152.

Dampney RA (1994): Functional organization of central pathways regulating the cardiovascular system. Physiol Rev 74:323–364.

Dampney RA, Coleman MJ, Fontes MA, Hirooka Y, Horiuchi J, Li YW, Polson JW, Potts PD, Tagawa T (2002): Central mechanisms underlying short- and long-term regulation of the cardiovascular system. Clin Exp Pharmacol Physiol 29:261–268.

Dampney RA, Polson JW, Potts PD, Hirooka Y, Horiuchi J (2003): Functional organization of brain pathways subserving the baroreceptor reflex: Studies in conscious animals using immediate early gene expression. Cell Mol Neurobiol 23:597–616.

Devinsky O, Morrell MJ, Vogt BA (1995): Contributions of anterior cingulate cortex to behaviour. Brain 118:279–306.

Eckberg DL, Sleight P (1992): Human Baroreflexes in Health and Disease. Oxford, UK: Oxford University Press.

Eisenberger NI, Lieberman MD (2004): Why rejection hurts: A common neural alarm system for physical and social pain. Trends Cogn Sci 8:294–300.

Etkin A, Egner T, Kalisch R (2011): Emotional processing in anterior cingulate and medial prefrontal cortex. Trends Cogn Sci 15:85–93.

Freedman LJ, Insel TR, Smith Y (2000): Subcortical projections of area 25 (subgenual cortex) of the macaque monkey. J Comp Neurol 421:172–188.

Friston K (1994): Functional and effective connectivity in neuroimaging: A synthesis. Hum Brain Mapp 2:56–78.

Friston KJ, Buechel C, Fink GR, Morris J, Rolls E, Dolan RJ (1997): Psychophysiological and modulatory interactions in neuroimaging. NeuroImage 6:218–229.

Gianaros PJ, Sheu LK (2009): A review of neuroimaing studies of stressor-evoked blood pressure reactivity: Emerging evidence for a brain-body pathway to coronary heart disease risk. NeuroImage 47:922–936.

Gianaros PJ, Derbyshire SW, May JC, Siegle GJ, Gamalo MA, Jennings JR (2005): Anterior cingulate activity correlates with blood pressure during stress. Psychophysiology 42:627–635.

Gianaros PJ, Jennings JR, Sheu LK, Derbyshire SW, Matthews KA (2007): Heightened functional neural activation to psychological stress covaries with exaggerated blood pressure reactivity. Hypertension 49:134–140.

Gianaros PJ, Sheu LK, Matthews KA, Jennings JR, Manuck SB, Hariri AR (2008): Individual differences in stressor-evoked blood pressure reactivity vary with activation, volume, and functional connectivity of the amygdala. J Neurosci 28:990–999.

Gianaros PJ, Sheu LK, Remo AM, Christie IC, Crtichley HD, Wang J (2009): Heightened resting neural activity predicts exaggerated stressor-evoked blood pressure reactivity. Hypertension 53:819–825.

Gianaros PJ, van der Veen FM, Jennings JR (2004): Regional cerebral blood flow correlates with heart period and high-frequency heart period variability during working-memory tasks: Implications for the cortical and subcortical regulation of cardiac autonomic activity. Psychophysiology 41:521–530.

Gizdulich P, Imholz BP, van den Meiracker AH, Parati G, Wesseling KH (1996): Finapres tracking of systolic pressure and baroreflex sensitivity improved by waveform filtering. J Hypertens 14:243–250.

Gray MA, Minati L, Harrison NA, Gianaros PJ, Napadow V, Critchley HD (2009a): Physiological recordings: Basic concepts and implementation in the fMRI scanner. NeuroImage 47:1105–1115.

Gray MA, Rylander K, Harrison NA, Wallin BG, Critchley HD (2009b): Following one's heart: Cardiac rhythms gate central initiation of sympathetic reflexes. J Neurosci 29:1817–1825.

Greicius MD, Krasnow B, Reiss AL, Menon V (2003): Functional connectivity in the resting brain: A network analysis of the default mode hypothesis. Proc Natl Acad Sci USA 100:253–258.

Guelen I, Westerhof BE, van der Sar GL, van Montfrans GA, Kiemeneij F, Wesseling KH, Bos WJ (2003): Finometer, finger pressure measurements with the possibility to reconstruct brachial pressure. Blood Press Monit 8:27–30.

Guyenet PG (2006): The sympathetic control of blood pressure. Nat Rev Neurosci 7:335–346.

Harrison NA, Gray MA, Gianaros PJ, Critchley HD (2010): The embodiment of emotional feelings in the brain. J Neurosci 30:12878–12884.

Heimer L, van Hoesen GW (2006): The limbic lobe and its output channels: Implications for emotional functions and adaptive behavior. Neurosci Biobehav Rev 30:126–147.

Hester R, Fassbender C, Garavan H (2004): Individual differences in error processing: A review and reanalysis of three event-related fMRI studies using the GO/NOGO task. Cereb Cortex 14:986–994.

Holroyd CB, Coles MG (2002): The neural basis of human error processing: Reinforcement learning, dopamine, and the error-related negativity. Psychol Rev 109:679–709.

Kamarck TW, Lovallo WR (2003): Cardiovascular reactivity to psychological challenge: Conceptual and measurement considerations. Psychosom Med 65:9–21.

Kamarck TW, Jennings JR, Debski TT, Glickman-Weiss E, Johnson PS, Eddy MJ, Manuck SB (1992): Reliable measures of behaviorally-evoked cardiovascular reactivity from a PC-based test battery: Results from student and community samples. Psychophysiology 29:17–28.

Kimmerly DS, O'Leary DD, Menon RS, Gati JS, Shoemaker JK (2005): Cortical regions associated with autonomic cardiovascular regulation during lower body negative pressure in humans. J Physiol 569:331–345.

Koski L, Paus T (2000): Functional connectivity of the anterior cingulate cortex within the human frontal lobe: A brain-mapping meta-analysis. Exp Brain Res 133:55–65.

Kroenke K, Spitzer RL, Williams JB (2001): The PHQ-9: Validity of a brief depression severity measure. J Gen Intern Med 16:606–613.

La Rovere MT, Pinna GD, Raczak G (2008): Baroreflex sensitivity: Measurement and clinical implications. Ann Noninvasive Electrocardiol 13:191–207.

Lane RD, Reiman EM, Axelrod B, Yun LS, Holmes A, Schwartz GE (1998): Neural correlates of levels of emotional awareness. Evidence of an interaction between emotion and attention in the anterior cingulate cortex. J Cogn Neurosci 10:525–535.

Lane RD, McRae K, Reiman EM, Chen K, Ahern GL, Thayer JF (2009a): Neural correlates of heart rate variability during emotion. NeuroImage 44:213–222.

Lane RD, Waldstein SR, Chesney MA, Jennings JR, Lovallo WR, Kozel PJ, Rose RM, Drossman DA, Schneiderman N, Thayer JF, Cameron OG (2009b): The rebirth of neuroscience in psychosomatic medicine. I. Historical context, methods and relevant basic science. Psychosom Med 71:117–134.

Lowe B, Grafe K, Zipfel S, Witte S, Loerch B, Herzog W (2004a): Diagnosing ICD-10 depressive episodes: Superior criterion validity of the Patient Health Questionnaire. Psychother Psychosom 73:386–390.

Lowe B, Kroenke K, Herzog W, Grafe K (2004b): Measuring depression outcome with a brief self-report instrument: Sensitivity to change of the Patient Health Questionnaire (PHQ-9). J Affect Disord 81:61–66.

Martin A, Rief W, Klaiberg A, Braehler E (2006): Validity of the Brief Patient Health Questionnaire Mood Scale (PHQ-9) in the general population. Gen Hosp Psychiatry 28:71–77.

McEwen BS, Gianaros PJ: Plasticity of the brain in relationship to stress. Annu Rev Med 62:431–445.

Mujica-Parodi LR, Korgaonkar M, Ravindranath B, Greenberg T, Tomasi D, Wagshul M, Ardekani B, Guilfoyle D, Khan S, Zhong Y, Chon K, Malaspina D (2009): Limbic dysregulation is associated with lowered heart rate variability and increased trait anxiety in healthy adults. Hum Brain Mapp 30:47–58.

Nagai Y, Critchley HD, Featherstone E, Trimble MR, Dolan RJ (2004): Activity in ventromedial prefrontal cortex covaries with sympathetic skin conductance level: A physiological account of a "default mode" of brain function. NeuroImage 22:243–251.

Nagai M, Hoshide S, Kario K (2010): The insular cortex and cardiovascular system: A new insight into the brain-heart axis. J Am Soc Hypertens 4:174–182.

Neafsey EJ (1990): Prefrontal cortical control of the autonomic nervous system: Anatomical and physiological observations. Prog Brain Res 85:147–165.

Neafsey EJ, Terreberry RR, Hurley KM, Ruit KG, Frysztak RJ (1993): Anterior cingulate cortex in rodents: Connections, visceral control functions, and implications for emotion. In: Vogt BA, Gabriel M, editors. Neurobiology of Cingulate Cortex and Limbic Thalamus: A Comprehensive Handbook. Boston, MA: Birkhauser.

O'Connor MF, Gundel H, McRae K, Lane RD (2007): Baseline vagal tone predicts BOLD response during elicitation of grief. Neuropsychopharmacology 32:2184–2189.

Obrist PA (1981): Cardiovascular Psychophysiology: A Perspective. New York, NY: Plenum Press.

Öngür D, Price J (2000): The organization of networks within the orbital and medial prefrontal cortex of rats, monkeys, and humans. Cereb Cortex 10:206–219.

Oppenheimer S (1993): The anatomy and physiology of cortical mechanisms of cardiac control. Stroke 24:I3–I5.

Oppenheimer SM, Gelb A, Girvin JP, Hachinski VC (1992): Cardiovascular effects of human insular cortex stimulation. Neurology 42:1727–1732.

Oppenheimer SM, Kedem G, Martin WM (1996): Left-insular cortex lesions perturb cardiac autonomic tone in humans. Clin Auton Res 6:131–140.

Palomero-Gallagher N, Mohlberg H, Zilles K, Vogt B (2008): Cytology and receptor architecture of human anterior cingulate cortex. J Comp Neurol 508:906–926.

Paus T (2001): Primate anterior cingulate cortex: Where motor control, drive, and cognition interface. Nat Neurosci Rev 2:417–424.

Paus T, Koski L, Caramanos Z, Westbury C (1998): Regional differences in the effects of task difficulty and motor output on blood flow response in the human anterior cingulate cortex: A review of 107 PET activation studies. Neuroreport 9:R37–R47.

Phillips ML, Drevets WC, Rauch SL, Lane R (2003): Neurobiology of emotion perception I: The neural basis of normal emotion perception. Biol Psychiatry 54:504–514.

Resstel LB, Correa FM (2006): Involvement of the medial prefrontal cortex in central cardiovascular modulation in the rat. Auton Neurosci 126–127:130–138.

Ridderinkhof KR, Ullsperger M, Crone EA, Nieuwenhuis S (2004a): The role of the medial frontal cortex in cognitive control. Science 306:443–447.

Ridderinkhof KR, van den Wildenberg WP, Segalowitz SJ, Carter CS (2004b): Neurocognitive mechanisms of cognitive control: The role of prefrontal cortex in action selection, response inhibition, performance monitoring, and reward-based learning. Brain Cogn 56:129–140.

Ruggiero DA, Mraovitch S, Granata AR, Anwar M, Reis DJ (1987): A role of insular cortex in cardiovascular function. J Comp Neurol 257:189–207.

Saha S (2005): Role of the central nucleus of the amygdala in the control of blood pressure: Descending pathways to medullary cardiovascular nuclei. Clin Exp Pharmacol Physiol 32:450–456.

Schlor KH, Stumpf H, Stock G (1984): Baroreceptor reflex during arousal induced by electrical stimulation of the amygdala or by natural stimuli. J Auton Nerv Syst 10:157–165.

Seeley WW, Menon V, Schatzberg AF, Keller J, Glover GH, Kenna H, Reiss AL, Greicius MD (2007): Dissociable intrinsic connectivity networks for salience processing and executive control. J Neurosci 27:2349–2356.

Spielberger C, Gorsuch R, Lushene R (1970): STAI Manual for the State-Trait Anxiety Inventory. Palo Alto, CA: Consulting Psychologists Press, Inc.

Spitzer RL, Kroenke K, Williams JB (1999): Validation and utility of a self-report version of PRIME-MD: The PHQ primary care study. JAMA 282:1737–1744.

Steptoe A, Sawada Y (1989): Assessment of baroreceptor reflex function during mental stress and relaxation. Psychophysiology 26:140–147.

Thayer JF, Lane RD (2009): Claude Bernard and the heart-brain connection: Further elaboration of a model of neurovisceral integration. Neurosci Biobehav Rev 33:81–88.

Thayer JF, Hansen AL, Johnsen BH (2010): The non-invasive assessment of autonomic influences on the heart using impedance cardiography and heart rate variability. In: Steptoe A, editor. Handbook of Behavioral Medicine. New York: Springer Science.

Treiber FA, Kamarck T, Schneiderman N, Sheffield D, Kapuku G, Taylor T (2003): Cardiovascular reactivity and development of preclinical and clinical disease states. Psychosom Med 65:46–62.

Ulrich-Lai YM, Herman JP (2009): Neural regulation of endocrine and autonomic stress responses. Nat Rev Neurosci 10:397–409.

Verberne AJM, Owens NC (1998): Cortical modulation of the cardiovascular system. Prog Neurobiol 54:149–168.

Verberne AJ, Lewis SJ, Worland PJ, Beart PM, Jarrott B, Christie MJ, Louis WJ (1987): Medial prefrontal cortical lesions modulate baroreflex sensitivity in the rat. Brain Res 426:243–249.

Vogt BA (2005): Pain and emotion interactions in subregions of the cingulate gyrus. Nat Rev Neurosci 6:533–544.

Vogt BA, Pandya DN (1987): Cingulate cortex of the rhesus monkey. II. Cortical afferents. J Comp Neurol 262:271–289.

Vogt BA, Laureys S (2005): Posterior cingulate, precuneal and retrosplenial cortices: Cytology and components of the neural network correlates of consciousness. Prog Brain Res 150:205–217.

Vogt BA, Finch DM, Olson CR (1992): Functional heterogeneity in cingulate cortex: The anterior executive and posterior evaluative regions. Cereb Cortex 2:435–443.

Vogt BA, Nimchinsky EA, Vogt LJ, Hof PR (1995): Human cingulate cortex: Surface features, flat maps, and cytoarchitecture. J Comp Neurol 359:490–506.

Wager T, van Ast V, Hughes B, Davidson M, Lindquist M, Ochsner K (2009a): Brain mediators of cardiovascular responses to social threat. II. Prefrontal-subcortical pathways and relationship with anxiety. NeuroImage 47:836–851.

Wager TD, Waugh CE, Lindquist MA, Noll DC, Fredrickson BL, Taylor SF (2009b): Brain mediators of cardiovascular responses to social threat. I. Reciprocal dorsal and ventral sub-regions of the medial prefrontal cortex and heart-rate reactivity. NeuroImage 47:821–835.

Wang JJ, Rao H, Wetmore GS, Furlan PM, Korczykowski M, Dinges DF, Detre JA (2005): Perfusion functional MRI reveals cerebral blood flow pattern under psychological stress. Proc Natl Acad Sci USA 102:17804–17809.

Wesseling KH, de Wit B, van der Hoeven GMA, van Goudoever J, Settels J (1995): Physiocal: Calibrating finger vascular physiology for Finapres. Homeostasis 36:67–82.

Westerhof BE, Gisolf J, Stok WJ, Wesseling KH, Karemaker JM (2004): Time-domain cross-correlation baroreflex sensitivity: Performance on the EUROBAVAR data set. J Hypertens 22:1371–1380.

Wong SW, Masse N, Kimmerly DS, Menon RS, Shoemaker JK (2007): Ventral medial prefrontal cortex and cardiovagal control in conscious humans. NeuroImage 35:698–708.

Yasui Y, Breder CD, Saper CB, Cechetto DF (1991): Autonomic responses and efferent pathways from the insular cortex in the rat. J Comp Neurol 303:355–374.